Embedding stochastic dynamics of the environment in spontaneous activity by prediction-based plasticity

Toshitake Asabuki[1]* and Claudia Clopath[1]*

[1] Department of Bioengineering, Imperial College London, London, UK.

*To whom correspondence should be addressed.

E-mail: c.clopath@imperial.ac.uk (C.C.); t.asabuki@imperial.ac.uk (T.A.)

Author Contributions: T.A. and C.C. conceived the study and wrote the paper. T.A. performed the simulations and data analyses.

Competing Interest Statement: The authors declare no competing interests.

Keywords: synaptic plasticity; recurrent spiking neural network; internal model; spontaneous activity; transition statistics

Abstract

The brain learns an internal model of the environment through sensory experiences, which is essential for high-level cognitive processes. Recent studies show that spontaneous activity reflects such learned internal model. Although computational studies have proposed that Hebbian plasticity can learn the switching dynamics of replayed activities, it is still challenging to learn dynamic spontaneous activity that obeys the statistical properties of sensory experience. Here, we propose a pair of biologically plausible plasticity rules for excitatory and inhibitory synapses in a recurrent spiking neural network model to embed stochastic dynamics in spontaneous activity. The proposed synaptic plasticity rule for excitatory synapses seeks to minimize the discrepancy between stimulus-evoked and internally predicted activity, while inhibitory plasticity maintains the excitatory-inhibitory balance. We show that the spontaneous reactivation of cell assemblies follows the transition statistics of the model's evoked dynamics. We also demonstrate that simulations of our model can replicate recent experimental results of spontaneous activity in songbirds, suggesting that the proposed plasticity rule might underlie the mechanism by which animals learn internal models of the environment.

Significance Statement

While spontaneous activity in the brain is often seen as simple background noise, recent work has hypothesized that spontaneous activity instead reflects the brain's learnt internal model. While several studies have proposed synaptic plasticity rules to generate structured spontaneous activities, the mechanism of learning and embedding transition statistics in spontaneous activity is still unclear. Using a computational model, we investigate the synaptic plasticity rules that learn dynamic spontaneous activity obeying appropriate transition statistics. Our results shed light on the learning mechanism of the brain's internal model, which is a crucial step towards a better understanding of the role of spontaneous activity as an internal generative model of stochastic processes in complex environments.

Introduction

The brain is thought to use its sensory experience to learn an appropriate internal model of the environment, which can improve perception and behavioral performance. (Merfeld et al., 1999; Lewald and Ehrenstein, 1998; Bell et al., 1997; Yasui and Young, 1975; Wolpert et al., 1995). Such learning is thought to be

fundamental to higher-order cognitive processes such as perception, decision making, and prediction of sensory stimuli. Recent computational and experimental evidence suggests that the brain's learned internal model may be reflected in spontaneous activity. For example, in the visual cortex of awake ferrets, spontaneous activity shows spatial similarity to activity elicited by natural scenes (Berkes et al., 2011). Furthermore, hippocampus generates sequential replay of place fields during rest and sleep (Wilson and McNaughton, 1994; Skaggs and McNaughton, 1996; Lee and Wilson, 2002). Such hippocampal replay occurs in a highly stereotyped temporal order, with the same sequence of replayed activities often observed across multiple events (Davidson et al., 2009; Diba and Buzsáki, 2007; Gupta et al., 2010; Wu and Foster, 2014).

Several computational studies have proposed variants of Hebbian plasticity rules for learning deterministic or even stochastic switching dynamics of replayed activities (Levy et al., 2001; Litwin-Kumar and Doiron, 2014; Triplett et al., 2018; Ocker and Doiron, 2019; Asabuki and Fukai, 2023). However, it has been challenging to extend these results to generate dynamic spontaneous activity obeying appropriate transition probabilities learned through sensory experience. Finding a plasticity rule which is capable of learning structured transitions in spontaneous activity could be instrumental for understanding the mechanism underlying cognitive processes in the brain.

In this paper, we propose a local biologically-plausible plasticity rule for learning the statistical transitions between assemblies in spontaneous activity. We use a recurrent spiking neural network model consisting of distinct excitatory and inhibitory populations. The proposed synaptic plasticity rule for excitatory synapses seeks to minimize the discrepancy between stimulus-evoked and internally predicted activity, while inhibitory plasticity maintains the excitatory-inhibitory balance. We explore the potential performance of our model by learning the Markovian transition statistics of evoked network states. Our results show that the trained model exhibits spontaneous stochastic transitions of cell assemblies, even after structured external inputs are removed. We show that the transition statistics of spontaneous activity show a striking similarity to those of the evoked dynamics.

To further validate our model, we compare the model behavior with recent experimental results in songbirds (Bouchard and Brainard, 2016), which show that the

uncertainty of upcoming states in a bird song modulates the degree of neural predictability. Our model replicates this experimental result, suggesting that the connectivity structure learned via the proposed plasticity mechanism could plausibly underly the songbird's learned internal model.

Results

Spontaneous replay of learnt stochastic sequences

While most studies have investigated plasticity mechanisms for learning random switching (Litwin-Kumar and Doiron, 2014; Triplett et al., 2018; Ocker and Doiron, 2019; Asabuki and Fukai, 2023) or deterministic transitions (Chadwick et al., 2015) between cell assemblies, our objective is to create a network model that spontaneously generates stochastic sequences of assemblies following synaptic plasticity. To that end, we first design a simple task whereby stimuli undergo stochastic transitions over time, and presentation of each stimulus increases excitatory drive to neurons targeted by that pattern (Fig.1a, top). We assume that a non-overlapping subset of excitatory network neurons receive its preferred stimulus (Fig. 1b). After learning, the network should replay stochastic sequences of assemblies with transitions that are statistically consistent with evoked dynamics, without relying on external stimuli (Fig.1a, bottom).

We examined the possible learning mechanisms of stochastic neural sequences with a recurrent spiking network. Our network model consists of excitatory (E) and inhibitory (I) model neurons (Fig. 1b). Only excitatory neurons are driven by external stochastic sequences. Initially, neurons in the network have random recurrent connections.

To learn a network model to obtain transition statistics of evoked dynamics, we proposed different local plasticity mechanisms for excitatory and inhibitory synapses. We assumed that only connections onto excitatory neurons were plastic (Fig. 1b), while all others (i.e., connections onto inhibitory neurons) were fixed. In the excitatory recurrent connectivity, all synaptic weights were modified to reduce the error between internally generated and stimulus-evoked activities (Fig. 1c, blue square). This plasticity rule is mathematically similar to that proposed in (Pfister et al., 2006; Urbanczik and Senn, 2014). Through this process, excitatory synapses that contribute to predicting neural activity will be strengthened, thereby increasing the similarity between spontaneous and evoked activity. Instead of

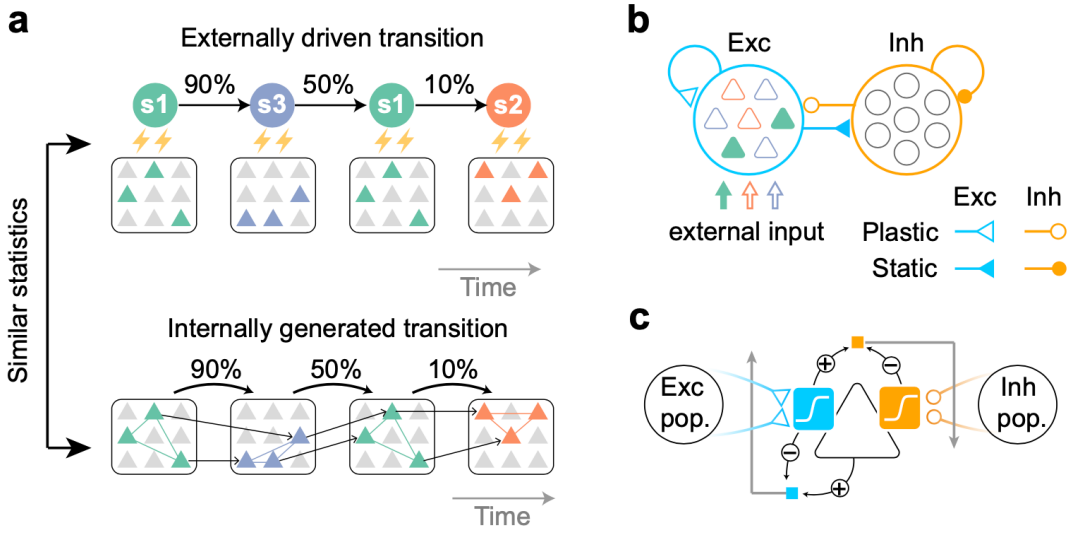

Figure 1. Task to be learned (a, top) An example of a task used to test the model. Stimulus patterns evolve in time according to structured transition probabilities. The presentation of each stimulus pattern activates the corresponding group of neurons. Recurrent connections are learned by synaptic plasticity (a, bottom). The learned network should replay assemblies spontaneously, where the transition statistics are consistent with the evoked stimuli. (b) A network model with distinct excitatory and inhibitory populations. Only excitatory populations are driven by external inputs. Only synapses that project to excitatory neurons are assumed to be plastic. (c) A schematic of the proposed plasticity rules. Excitatory (blue) and inhibitory (orange) synapses projecting to an excitatory neuron (triangle) obey different plasticity rules. For excitatory synapses, errors between internally driven excitation (blue sigmoid) and the output of the cell provide feedback to the synapses and modulate plasticity (blue square). All excitatory connections seek to minimize such errors. For inhibitory synapses, the error between internally driven excitation (blue sigmoid) and inhibition (orange sigmoid) should be minimized to maintain excitatory inhibitory balance (orange square).

predicting the firing rate of neurons, the inhibitory synapses were modified to predict the recurrent excitatory potential (Fig. 1c, orange square). This inhibitory plasticity is crucial for the network to maintain excitatory-inhibitory balance and generate spontaneous replay of stochastic assembly sequences, as we will see later. All feedforward connections were fixed and receptive fields were preconfigured. Finally, as in previous studies (Asabuki and Fukai, 2023), parameters of the response function are regulated according to the activity history of individual neurons (Methods). This regulation maintains the appropriate dynamic range of activities irrespective of the strength of external stimuli.

To examine how external stochastic sequences can influence network wiring, we trained a network model driven by stochastic external inputs. These inputs were generated by first-order Markovian chains with three 200ms long states,

governed by fixed transition probabilities (Fig. 2a). During training, excitatory synapses were modified much quicker than inhibitory synapses (Fig.2b). This difference in plasticity timescales follows from the nature of our learning rules: the wiring of excitatory synapses is reorganized by external stimuli, while inhibitory synapses only change to rebalance excitation. As such, excitatory plasticity in our model occurs before inhibitory plasticity, consistent with the experimental results (D'amour JA and Froemke, 2015). We then asked how plasticity affects the neural dynamics by comparing the spontaneous activities of the network before and after learning. Here, we simulated spontaneous activity by replacing the temporally structured stimulation (i.e., the Markovian chain in Fig.2a) with constant background input. Further, all synapses were kept fixed during spontaneous activity.

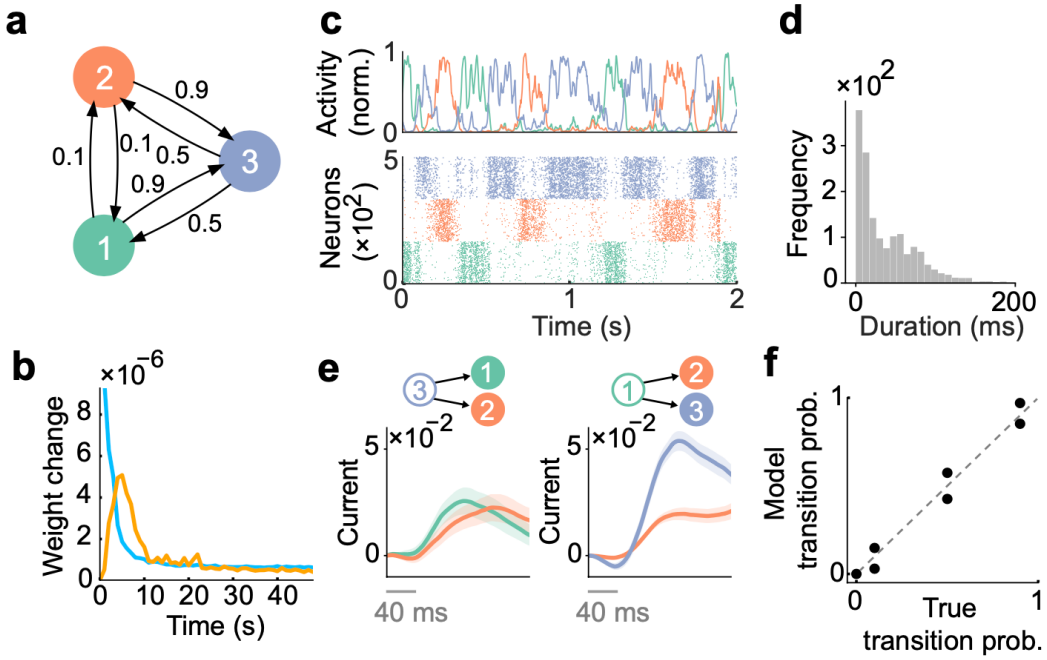

Figure 2. Spontaneous replay of stochastic transition of assemblies. (a) First, we considered a simple stochastic transition between three stimulus patterns. (b) Dynamics of weight change via plasticity. Excitatory synapses (blue) converged quicker than inhibitory synapses (orange). (c) Example spontaneous assembly reactivations (top) and raster plot (bottom) of the learned network are shown. Colors indicate the corresponding stimulus patterns shown in a. (d) Distribution of assembly reactivations. (e, left) The network currents to assembly 1 (green) and assembly 2 (orange) immediately after the reactivation of assembly 3 ceased. Both currents were similar in magnitude. (e, right) Currents to assembly 2 (orange) and assembly 3 (blue) immediately after the reactivation of assembly 1 ceased. The current to assembly 3 was stronger than that to assembly 2. (f) Relationship between the transition statistics of stimulus patterns and that of replayed assemblies. The spontaneous activity reproduced transition statistics of external stimulus patterns.

Before learning, due to uniform initial connectivity, all excitatory neurons showed synchronous and spatially unstructured spontaneous activity (Supplementary Fig.1). However, after learning, three cell assemblies emerged in the network, each of which encoded one external stimulus. Sequences of these cell assemblies were replayed stochastically in spontaneous activity (Fig. 2c), and durations of given assembly reactivations were biased toward shorter durations but distributed broadly (Fig.2d).

We next asked whether or not the statistics of assembly switching were influenced by the temporal structure of the external sequence received by the network while it was learning. Since each assembly reactivation was contingent upon previous assembly, statistics of external sequence may influence the strength of synaptic currents via recurrent connectivity. To test this prediction, we first investigated how spontaneous reactivation of assembly 3 drives the subsequent assemblies (i.e., assemblies 1 and 2). Immediately after the reactivation of assembly 3 ceased, currents onto both subsequent assemblies increased gradually, without showing significant difference (Fig.2e, left). This is due to the fact that state 1 and 2 are structurally symmetrical in our setting (Fig.2a). We then asked how reactivation of assembly 1 drives the subsequent assemblies (i.e., assemblies 2 and 3). We note that the transition probabilities in the stimulus patterns were biased towards state 3 in this case (Fig.2a). Consistent with this bias between transition probabilities, we found that assembly 3 was driven much strongly than assembly 2 (Fig.2e, right). These results suggest that the temporal statistics of the trained external sequence influence the strength of synaptic currents that drive each assembly. We then quantified the similarity between the transition statistics of stimulus patterns and that of the replayed assemblies. We defined the transition probabilities between assemblies by simply counting the occurrence of switching events over all possible pairs of assemblies (Methods). Comparison between transition probabilities of stimulus patterns and that of the reactivated assemblies revealed a clear alignment of temporal statistics (Fig.2f).

In summary, the plasticity rules in our model learn the transition statistics of evoked patterns while maintaining excitation-inhibition balance. Our results show that the this prediction-based plasticity rule allows the model to learn and spontaneously replays the transition statistics of evoked patterns.

Learned excitatory synapses encode transition statistics

To further understand the mechanism underlying the statistical similarity between the evoked patterns and spontaneous activity, we next asked how the transition statistics of stimulus patterns can influence network wiring. Over the course of training, the average weights of connections in each of the 3 cell assemblies increased gradually and converged to a strong value (Fig.3a middle and Fig.3b, top), indicating the formation of assemblies. On the other hand, we found that the average weights between each pair of assemblies decreased settled at different stationary values (Fig.3a, right and Fig.3b, bottom). After training, we reasoned that the transition probabilities between states should be encoded exclusively via between-assembly connections, as none of the states in the Markovian chain have self-transitions. To test this prediction, we first compared the average between-assembly connection matrix (Fig.3a, right) and the ground truth transition aligned well to the ground truth probabilities (Fig.3d). These results indicate that

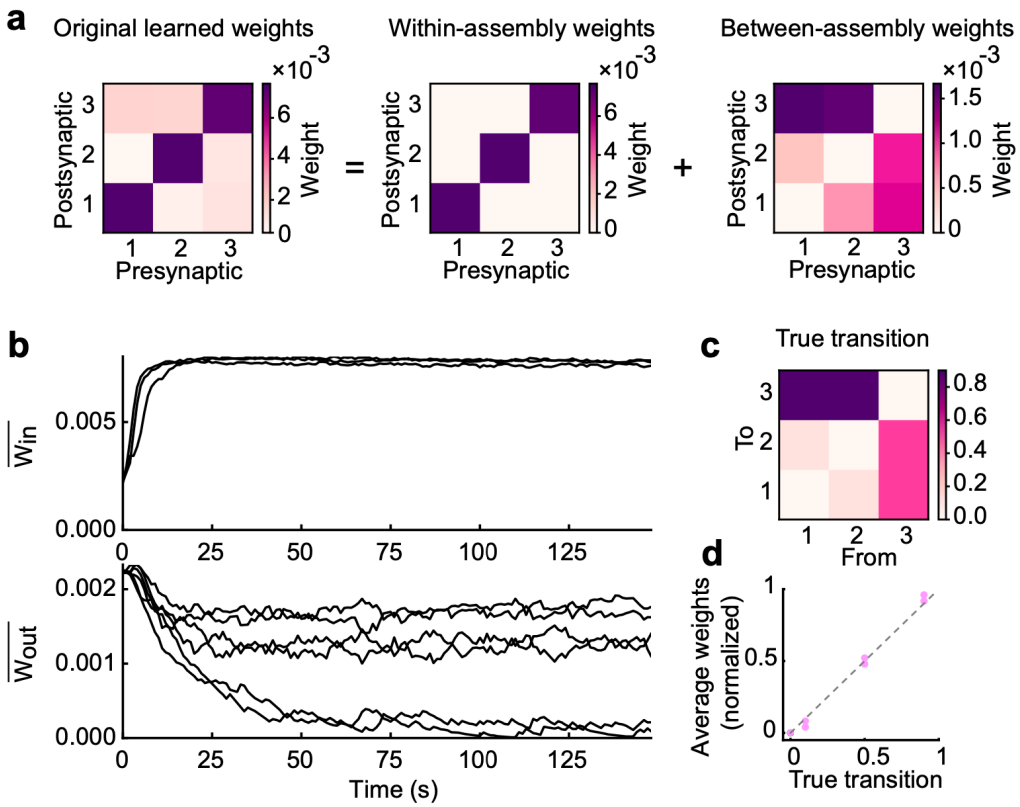

Figure 3. Learned excitatory synapses encode transition statistics. (a) A 3 by 3 matrix of excitatory connections, learned with the task in Fig.2a (left). The matrix can be decomposed to within- (middle) and between-assembly connections (right). (b) Strength of within- (top) and that of between-assembly excitatory synapses (bottom) during learning are shown. (c) True transition matrix of stimulus patterns. (d) Relationship between the strength of excitatory synapses between assemblies and true transition probabilities between patterns.

the network learns the temporal statistics of sequences by modifying the structure of inter-assembly excitatory connections.

The above analysis of excitatory weights revealed its crucial role in learning transition probabilities. Next, we examined the role of inhibitory plasticity in our model's function. To do so, we first simulated the network with fixed inhibitory weights performing the same task shown in Figure 2. We found that such a model exhibited spontaneous activity with blurred assembly structures compared to the original model (Supplementary Fig.2a). Furthermore, the transition probabilities between replayed assemblies in this case did not show clear alignment with true transition (Supplementary Fig. 2b), though the excitatory weights reached values which did encode transitions (Supplementary Fig. 2c, d). These results suggest that maintenance of EI balance through inhibitory plasticity is necessary for generating structured spontaneous activity, even if excitatory connections learn transition probabilities.

Network can adapt fast to task switching

In the above results, transitions between stimulus patterns obeyed fixed transition probabilities. We then wondered how the network learning would be affected if transition structures of stimulus patterns changed over time. To test such a scenario, we considered a case where the transition matrix in a Markovian chain switches between the first half and the second half of the learning phase (Supplementary Fig. 3a). We will refer these matrices as task1- and task2-matrix, respectively, and examine whether switching of transition matrixes influences the connectivity. During the first half of learning phase, between-assembly connections converged to certain values to encode task1-matrix (Supplementary Fig. 3b, bottom, 0-500 seconds). However, such stable connectivity reorganized quickly once the imposed task was switched to task2-matrix (Supplementary Fig. 3b, bottom, 500-1,000 seconds). Note that in contrast to between-assemblies connections, within-assembly connections did not show such reorganization (Supplementary Fig. 3b, top). These results indicate that our model adapted to the second task even if distinct assembly structures were already formed during the first task.

To further understand how the model adapts to the new task, we next asked how error terms in excitatory and inhibitory plasticity (Eqs.11 and 13) change through

learning. As expected, the low-pass filtered errors $\mathrm{PE}^{\mathrm{exc}}$ and $\mathrm{PE}^{\mathrm{inh}}$ decreased as the network trained on task1 (Supplementary Fig.3c, 0-500 seconds). However, once the task was switched, errors showed an abrupt increase followed by a gradual decrease as the network learned the second task (Supplementary Fig.3c, 500-1,000 seconds; Supplementary Fig.3d). Consistent with the previous result (Figure 2b), the peak of inhibitory error occurred delayed after that of excitatory one in each task (D'amour JA and Froemke, 2015; Vogels et al., 2011) (Supplementary Fig. 3d). In summary, our model is also capable of task switching, via the reorganization of its weight structures through continuing plasticity.

The network can learn complex stochastic sequences

So far, we have considered the capabilities of our model in regard to the relatively simple class of stochastic dynamics. In particular, the task we considered above contains only three states, and the transition structure was symmetric. In a realistic sequence, like the song of a bird, transition statistics are typically heterogeneous and more structured. To evaluate the model performance over a wide variety of structures, we now consider a transition diagram with more complex structure (Fig.4a). Despite its complex structure, the learned network showed spontaneous reactivations of all assemblies evoked during learning (Fig.4b), and the transition dynamics between these assemblies were governed by learned transition probabilities (Fig.4c). Indeed, the learned weight structures were consistent with the transition probabilities between states as we have seen in simpler task (Supplementary Fig.4).

Recent experimental studies which examined temporal community structure (i.e., highly structured graph structure consisting of clusters of densely interconnected nodes; Fig.4d) found that human subjects tend to associate a given visual stimulus with other stimuli within the same “community” (Schapiro et al., 2013; Pudhiyidath et al., 2022). To investigate whether the model can learn to associate states within a stimulated community, we first trained the network with a stochastic sequence of inputs, generated by a random walk over graph with temporal community structure (Fig.4d). The learned model showed stochastic assembly transition during spontaneous activity (Fig.4e) relying on the appropriate weight structure (Fig.4f). Although transition occurred between all pairs of assemblies, transitions between connected states in the diagram occurred much frequently than transitions between disconnected states (Fig.4g). This is because plasticity formed

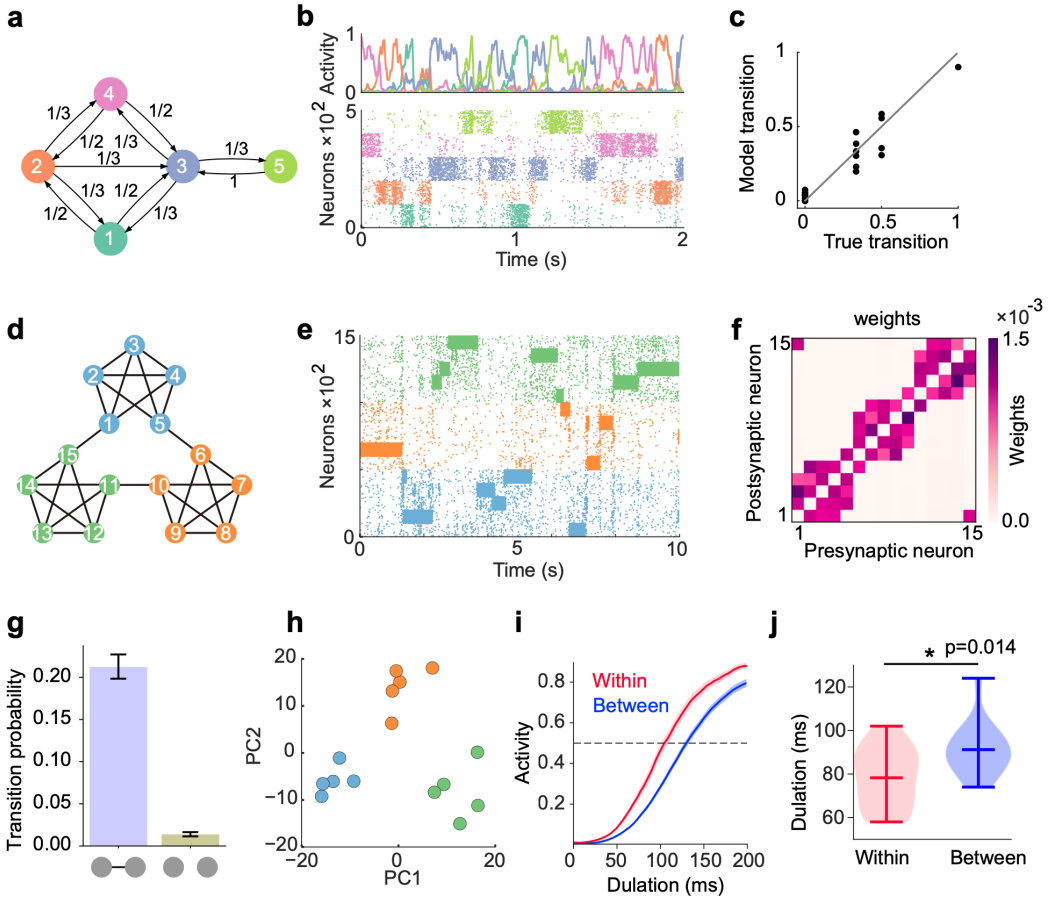

Figure 4. Learning complex structures. (a) Transition diagram of complex task. (b) Spontaneous activity of learned network. (c) Transition statistics of assemblies reproduce true statistics. (d) Transition diagram of temporal community structure. (e) Raster plot of spontaneous activity of the network trained over structure shown in (d). (f) Structure of learned excitatory synapses encode the community structure. (g) Spontaneous transition between assemblies connected in the diagram shown in d occurs much frequent than disconnected case. (h) Low dimensional representation of evoked activity patterns shows high similarity with community structure. (i) Time courses of replayed activities transitioning within (red) and between (blue) communities. (j) Comparison of mean durations in (i). P-value was calculated by two-sided Welch's t-test.

strong excitatory connections between assemblies with nonzero transition probabilities, as shown in Figure 4f.

In human participants, low-dimensional representations of evoked activities in different cortical regions have been reported to show clusters consistent with the structure of communities (Schapiro et al., 2013). To test whether our model could reproduce such representation of communities, we analyzed the low-dimensional representation of evoked activities in our model by applying principal component analysis (PCA) (see Methods). Such analysis revealed that the representation of stimulus patterns were grouped together into clusters or communities of mutually

predictive stimuli, consistent with the experimental results (Fig.4h). We found that the clustered representations still exist even if the input sequences were scrambled after learning (Supplementary Fig.5), indicating that this result does not rely on the stimulus protocol, but instead on the learned weights.

We further asked whether within- and between-community reactivations showed any differences in terms of their behavior. To this end, we perturbed an assembly corresponding to non-boundary states in the first community (states 2-4 in the transition diagram shown in Fig.4d) and monitored the behavior of subsequent autonomous network activities. According to the above results, we expect that within-community reactivations should occur quicker than between-community assemblies, due to strong within-community coupling. To test this hypothesis, we calculated the duration from the end of the perturbation until subsequent activity reached a certain threshold (Fig.4i). As expected, the transition to within-community states showed much shorter durations than to between-community case (Fig.4j), indicating that between-community transition occurred with much slower time scale compared to within-community case. Together, these results indicate that our network can learn complex temporal structures in spontaneous activity and reproduce the neural representation of the temporal community structure observed in the experiment.

Network dynamics consistent with recorded neural data of songbird

Finally, we tested whether the spontaneous activity in our model resembles recorded neural activity of HVC in Bengalese finch (Bf). Bf learns songs composed of multiple stereotyped short sequences, or syllables. The transitions between these syllables can be described via Markovian process with varying levels of certainty. Intuitively, given one syllable in a bird song, precise prediction about the neural response to the next syllable can be made if the transition from that syllable is highly certain, while imprecise transitions will lead to imprecise predictions about the neural response. Indeed, recent experimental study reported that uncertainty of upcoming syllables in a Bf song modulates the degree of predictability of subsequent neural activation (poststimulus activity; PSA) in HVC (Bouchard and Brainard, 2016). We sought to test whether our model would exhibit a similar property. To this end, we analyzed the behavior of a network model that had already learned the task (shown in Figure 4a). The transition structure we chose is relatively simple compared to the real song of a Bf, yet captures

measured features of bird songs (i.e., both structures consist of highly certain and less-certain transitions). In the experiment, similarities were calculated between the trial-averaged PSA following a short sequence of stimuli, and the response to an isolated stimulus. To mimic this experimental design, we measured stimulus-triggered averages of our autonomous network activity as a proxy for PSA (Fig.5a). To examine how uncertainty of state transitions in a sequence influence predictive strength in network activity, we first calculated the Pearson correlation coefficient between PSA and responses to next states in a sequence. We will refer to such correlations as “next-state correlations”. Note that if there were multiple next-states from a given state, all correlations corresponding to that state were averaged. We further calculated the correlation between PSA and responses to other states that did not follow the given state (“other-state correlations”). Similar to the next-state correlations, other-state correlations were averaged over all disconnected states from each state. We then compared next-state correlations and other-state correlations between highly certain (Fig.5b, left) and less-certain (Fig.5b, right) transitions. Here, highly certain transitions refer to those which have a transition probability greater than 1/2. Other transitions were classified as less-certain transitions. Consistent with experimental results, next-state correlations were significantly greater than other-state correlations in the highly certain case (Fig.5b, left). This correlation difference was less significant in less-certain case (Fig.5b, right). These results indicate that transition uncertainty modulated the degree to which PSA is predictive of upcoming states.

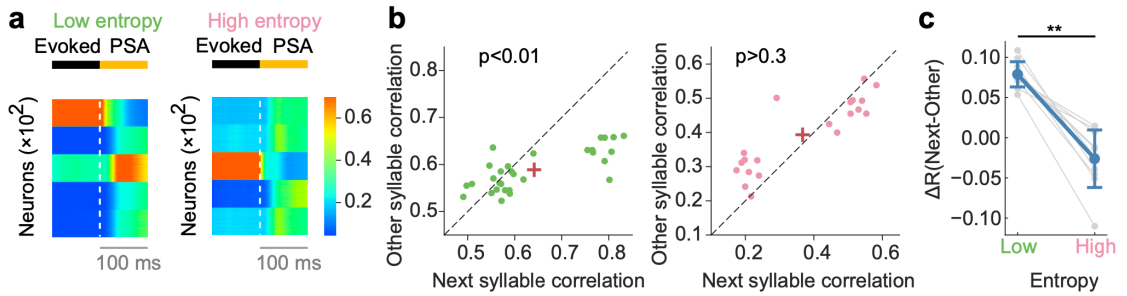

Figure 5. Network dynamics consistent with recorded neural data of songbird (a) Example post-stimulus activity (PSA) for low- (left) and high-entropy (right) transition cases. (b) Comparison of correlation coefficients between PSA and evoked single-syllable responses for next syllables and other syllables. For low entropy transition case, the next-syllables correlations were significantly higher than other-syllables correlations ($p < 0.01$, Wilcoxon signed-rank test) (left). In contrast, such correlation coefficients showed no significant difference for high entropy transition case ($p > 0.3$, Wilcoxon signed-rank test) (right). Red crosses are mean. (c) The difference in correlation coefficients between next and other syllables (ΔR) was significantly greater for low entropy transitions than for high entropy transitions ($p < 0.01$, two-sided Welch’s t-test).

We performed a more direct comparison of predictive strength by measuring the difference between two types of correlations (i.e., next- and other-state correlations) over multiple levels of transition uncertainty. Here, for each state, next-state correlation was subtracted by other-state correlation. Transition uncertainties were quantified by calculating the conditional entropy of transition probabilities of stimulus patterns. Note that a higher value of entropy indicates less-certain transition, and vice versa. As expected, correlation differences increased as entropy decreased (Fig.5c), indicating that the predictive strength of network PSA was larger for low-entropy transitions (i.e., highly certain transitions) than for high-entropy transitions (i.e., less-certain transitions). What is the underlying mechanism of such predictability differences? Although each trial of assembly perturbation lead to subsequent reactivation of one of the assemblies, trial-averaged activities (i.e., PSAs) marginalized all possible transitions in the transition diagram (Fig.5a). Due to this averaging process, similarities between PSA and stimulus-evoked activities increases if conditional entropy is low (i.e., certain transition), and vice versa. Overall, our results suggest that our model learns transition statistics of stimulus patterns, with transition uncertainty influencing predictive strength in the network activity.

Discussion

Understanding how the brain learns internal models of the environment is a challenging problem in neuroscience. In this study, we proposed synaptic plasticity rules for learning assembly transitions via sensory experiences. Our excitatory plasticity aims at minimizing the error between sensory-evoked and internally generated predictions of upcoming activity. We showed that the network learns the appropriate wiring patterns to encode the transition structure of states, and thus exhibits stochastic transitions between assemblies in spontaneous activity. We further showed that appropriate replay of stochastic transitions requires both excitatory and inhibitory plasticity. These plasticity rules showed a clear division of labor. For excitatory synapses, the connectivity learns transition probabilities during the evoked phase, and inhibitory plasticity seeks to maintain the excitatory-inhibitory balance. We showed that network excitatory plasticity alone cannot account for stochastic replay of learned activity, even if excitatory synapses learn an appropriate structure.

Variants of the Hebbian plasticity rule have been widely used to learn the precise order of sequential reactivations. For example, a rate-based Hebbian rule has been proposed to generate trajectories along a chain of metastable attractors, each corresponding to a reactivation of a single network state (Fonollosa et al., 2015). Another proposed mechanism is that the transitions are governed by theta oscillations, which form a temporal backbone of the sequential reactivation of assemblies (Chadwick et al., 2015). Despite the successes of these Hebbian rules in learning precise order in sequences, plasticity rules that learn structured transition probabilities and replay them in spontaneous activity were still unknown.

How does our plasticity mechanism differ from the Hebbian rule? In the Hebbian rule, synaptic strength is potentiated as long as pre- and postsynaptic neurons show correlated activities. Due to this nature of the Hebbian rule, after sufficient potentiation, synapses reach a predefined upper limit, making the strength uniform among strong synapses (Kempter et al., 1999; Song et al., 2000; Masquelier et al., 2008). Such connectivity is useful when the network learns deterministic sequences, but it alone is insufficient to learn transition probabilities. In contrast, our proposed model aims at predicting the evoked activities by internally generated dynamics, so that learning ceases when the prediction error is sufficiently minimized. This mechanism results in learned synaptic distributions that are not uniform as observed in STDP, but rather converge to values proportional to the transition probabilities between assemblies (as shown in Figure 3b).

The proposed mechanism of learning stochastic transitions between cell assemblies may offer several advantages over deterministic transitions, as suggested by previous studies. One possibility is that the internal dynamics of stochastic transitions can be used as prior knowledge about the structure of the world. In particular, the learned information about the transition statistics can be used to make probabilistic predictions about upcoming sensory events. It may also provide a flexible representation of the environment. In a deterministic case, assemblies are replayed in a fixed temporal order, which may make the network susceptible to noise or unexpected changes in the environment. In contrast, stochastic transitions may allow the network to generate rich repertoires of representations that could provide flexible computation against an uncertain environment.

In reinforcement learning (RL), balancing the tradeoff between exploration and exploitation to maximize a long-term reward signal is one of the most challenging

problems. While both exploration and exploitation phases are crucial in RL, exploration is often much more difficult. This difficulty arises from the fact that exploration is especially important when the agent does not have an optimal policy. One way in which the agent might bypass or speed up this exploration phase is through prior knowledge of the environment's transition statistics. Furthermore, learning transition statistics as an internal model may be beneficial when an agent solves a task in an environment where the reward distribution is sparse. Having an internal model of the transition statistics may allow an agent to predict the expected value of the future reward for taking a particular action in a given state. However, the relationship between the reward-based plasticity rule and our proposed rule still needs further study.

Our model results were also compared to experimental results of sequence predictability in a songbird. Recent experiments have shown that the predictive uncertainty of the upcoming stimulus modulates the degree of similarity between stimulus-evoked and post-stimulus autonomous activity in the HVC of the Bengal finch (Bouchard and Brainard, 2016). However, the underlying mechanism is still unknown. Here, we have shown that a stochastic state transition in spontaneous activity can explain such a dependence of activity similarity on stimulus uncertainty. Our model predicts that the PSA reflects a trial average of stochastic transitions of evoked activity from a given stimulus. Trial-averaged neural activity washes out the variability of all possible realizations of the stochastic transition. Thus, PSA of an uncertain stimulus results in a combination of multiple transitions, leading to activity less similar than that evoked by a single stimulus. Several studies have shown that Hidden Markov Models or other statistical methods could account for the transition statistics in bird song (Kogan and Margoliash, 1998; Katahira et al., 2011). However, our study suggests that trial averaging operations can influence the degree of similarity between stimulus-evoked and post-stimulus activity.

Although we have shown that the proposed model can learn Markovian transitions, several studies suggest that animals often exhibit behaviors with non-Markovian or hierarchical statistics (Seeds et al., 2014; Berman et al., 2016; Jovanic et al., 2016; Jin and Costa, 2015; Geddes et al., 2018; Markowitz et al., 2018; Kato et al., 2015; Kaplan et al., 2020). In principle, our learning rule cannot be applied to learning non-Markovian transitions, since it only learns local transitions between states (Brea et al., 2013). Another limitation of our model is that it cannot

learn transition statistics if the states are separated in time. Both of these problems could be solved by considering working memory (WM) (Baddeley, 1992; Miller and Cohen, 2001) in an activity-dependent (Funahashi et al., 1989; Goldman-Rakic, 1995; Fuster and Alexander, 1971; Amit and Brunel, 1997) or activity-silent manner (Mongillo et al., 2008; Barak and Tsodyks, 2014; Zucker and Regehr, 2002; Erickson et al., 2010). Clarifying the relationship between the proposed prediction-based plasticity rule and plasticity rules that support memory traces, such as short-term plasticity, will warrant future computational studies.

Our work sheds light on the learning mechanism of the brain's internal model, which is a crucial step towards a better understanding of the role of spontaneous activity as an internal generative model of stochastic processes in complex environments.

Methods

Our recurrent neural networks consist of N_E excitatory and N_I inhibitory neurons. During learning, the membrane potentials of neuron at time t with external current I_i^{ext} were calculated as follows:

$$u_i^E(t) = \sum_{j=1}^{N_E} W_{ij}^{EE} x_j^E(t) - \sum_{k=1}^{N_I} W_{ik}^{EI} x_k^I(t) + I_i^{\mathrm{ext}}(t), \qquad (1)$$

$$u_i^I(t) = \sum_{j=1}^{N_E} W_{ij}^{IE} x_j^E(t) - \sum_{k=1}^{N_I} W_{ik}^{II} x_k^I(t), \qquad (2)$$

where u_i^E and u_i^I are the membrane potential of i-th excitatory and inhibitory neuron, respectively (see Table 1 for the list of variables and functions). The strength of external input I_i^{ext} takes the value 1 if stimulus pattern targets neuron i was presented and 0 otherwise. This structured external input was replaced to constant inputs I_i^{const} of value 0.3 during spontaneous activity. We will describe the details of stimulus patterns later. $W_{ij}^{ab}(a, b = E; I)$ is a recurrent connection weight from j-th neuron in population b to i-th neuron in population a. All neurons were connected with a coupling probability of $p = 0.5$. Initial value of

synaptic weights W_{ij}^{ab} were uniformly set to $0.1/\sqrt{pN_b}$ if $a = E$ and $1/\sqrt{pN_b}$ if $a = I$. x_i^a is a postsynaptic potential evoked by i-th neuron in population a, which will be described later.

Spiking of each neuron model in population E was modeled as an inhomogeneous Poisson process with instantaneous firing rate f_i^{E} with a dynamic sigmoidal response function φ with parameters of slope β and threshold θ as:

$$f_i^{\mathrm{E}} = \varphi(u_i^E; h_i) \equiv \varphi_0 \left[1 + \exp[g\beta(h_i)(-u_i^E + g\theta(h_i))]\right]^{-1}, \quad (3)$$

where φ_0 is the maximum instantaneous firing rate of 50 Hz and $g = 2$. The slope β and threshold θ of sigmoidal function of population E was regulated by the memory trace h_i as:

$$\beta(h_i) = {h_i}^{-1}\beta_0 \qquad (4)$$

$$\theta(h_i) = h_i\theta_0 \ , \qquad (5)$$

where the values of constant parameters are $\beta_0 = 5$ and θ_0 =1. The memory trace tracks the maximum value of the short history of membrane potential u_i^E as

$$\begin{aligned} \dot{h}_i &= -{\tau_h}^{-1}h_i, \quad \text{if } h_i > u_i^E, \\ h_i &\leftarrow u_i^E, \quad \text{otherwise,} \end{aligned} \qquad (6)$$

where $\tau_h = 10$ s is a time scale of memory trace. Inhibitory neurons' firing rate were assumed to be calculated with static sigmoidal function as:

$$f_i^{\mathrm{I}} = \hat{\varphi}(u_i^I) \equiv \varphi_0\left[1 + \exp[\beta_0(-u_i^I + \theta_0)]\right]^{-1}, \qquad (7)$$

Where the maximum instantaneous firing rate φ_0 was assumed to be same with that of excitatory neurons (i.e., 50 Hz). The parameters β_0 and θ_0 are the constant values already appeared in Eqs. (4) and (5).

Neuron i in population a generates a Poisson spike train at the instantaneous firing rate of f_i^{a}. Let us describe the generated Poisson spike trains as:

$$X_i^a(t) = \sum_{t' \in t_i^a} \delta(t - t'), \qquad (8)$$

where δ is the Dirac's delta function and t_i^a is the set of time of the spikes of the neuron. The postsynaptic potential evoked by the neuron (i.e., x_i^a) was then calculated as:

$$\tau_s \dot{I}_i^a = -I_i^a + \frac{1}{\tau} X_i^a \qquad (9)$$

$$\dot{x}_i^a = -\frac{x_i^a}{\tau} + x_0 I_i^a, \qquad (10)$$

where $\tau_s = 5$ms, τ = 15 ms, and $x_0 = 25$.

The learning rules

All excitatory synaptic connections onto excitatory neurons obeyed the following plasticity rule to predict the activity of postsynaptic neurons as:

$$\Delta W_{ij}^{EE} = \epsilon[f_i^{\mathrm{E}} - y_i^{\mathrm{E}}] \cdot x_j^E, \qquad (11)$$

where y_i^{E} is a recurrent prediction of a firing rate, defined as:

$$y_i^{\mathrm{E}} = \hat{\varphi}\left(\sum_{j=1}^{N_E} W_{ij}^{EE} \cdot x_j^E\right), \qquad (12)$$

where the function $\hat{\varphi}(\cdot)$ is the static sigmoid function defined in Eq.7. In this study, the learning rate was set to $\epsilon = 10^{-4}$ in all simulations.

The inhibitory synapses onto excitatory neurons were plastic according to the following rule:

$$\Delta W_{ij}^{EI} = \epsilon[y_i^{\mathrm{E}} - y_i^{\mathrm{I}}]x_j^I, \qquad (13)$$

where y_i^{I} was the total inhibitory input onto postsynaptic neuron:

$$y_i^{\mathrm{I}} = \hat{\varphi}\left(\sum_{j=1}^{N_I} W_{ij}^{EI} \cdot x_j^I\right). \qquad (14)$$

Through this inhibitory plasticity, inhibitory synapses were modified to maintain excitatory-inhibitory balance in all excitatory neurons.

Table1. Definition of variables and functions.

$u_i^E,\ u_i^I$	Membrane potentials
$x_j^E,\ x_k^I$	Postsynaptic potentials
X_i^a	Poisson spike train generated by network neurons
$W_{ij}^{EE},\ W_{ik}^{EI},\ W_{ij}^{IE},\ W_{ik}^{II}$	Recurrent connections
I_i^{ext}	External current elicited by stimulus presentation
I_i^E, I_i^I	Synaptic currents generated by network neurons
$f_i^{\mathrm{E}},\ f_i^{\mathrm{I}}$	Instantaneous firing rates
$y_i^{\mathrm{E}},\ y_i^I$	Recurrent predictions
h_i	Memory trace

φ	Dynamic sigmoidal function
$\hat{\varphi}$	Static sigmoidal function
$\mathrm{PE}^{\mathrm{exc}}$, $\mathrm{PE}^{\mathrm{inh}}$	Filtered prediction errors

Table2. Parameter settings.

p	Connection probability	0.5
g	Gain parameter in sigmoid function	2
N_E, N_I	Network size	500, 500 (1500,1500 in Figs 5e-j)
ϵ	Learning rate	10^{-4}
τ_s	Synaptic time constant	5 ms
τ	Membrane time constant	15 ms
β_0, θ_0	Parameters for sigmoid	5, 1
τ_h	Time constant of memory trace	10 s
φ_0	Maximal firing rate	50 Hz
x_0	Scaling factor of synaptic current	25
τ_{avg}	Time constant for low-pass filtering the error	30 s
I_i^{const}	Constant external current during spontaneous activity	0.3

Simulation details

The parameters used in the simulations are summarized in Table 2. All simulations were performed in customized Python3 code written by TA with numpy 1.17.3 and scipy 0.18. Differential equations were numerically integrated using a Euler method with integration time steps of 1 ms.

Stimulation protocols

In all simulations, each stimulus patterns had a duration of 200 ms and were presented without inter-pattern interval. We assumed each neuron in a network was stimulated by one of stimulus patterns and targeted assemblies were not overlapped. Presentation of each pattern triggers excitatory current to its targeted neurons of strength 1 and zero otherwise. During spontaneous activity, stimulus patterns were replaced with constant background input I_i^{const} for all excitatory neurons. In Figure 5, we assumed all excitatory neurons receive both structured

and constant background inputs over whole period.

Calculation of transition probabilities in spontaneous activity

In Figs. 2f, 4c, and 4g, we first calculated the population average of the instantaneous firing rates of all neurons in each assembly, during spontaneous activity. We will term such activities as assembly activities. We then defined the assembly reactivations by events that the assembly activities exceeded the threshold of which the value 50% of maximum value of each assembly activities. Transition probabilities between assemblies across all possible pairs were then calculated by counting the occurrences of reactivation of the subsequent assembly within 100 ms of the end time of reactivation of the preceding assembly. In Fig. 2d, durations of each assembly reactivation event were defined as a period during each assembly activation exceeded threshold.

Calculation of weight changes

In Fig.2b, the weight changes were calculated every 2 s for excitatory and inhibitory synapses as:

$$\Delta \boldsymbol{W}^{\mathrm{EE}}(t) \coloneqq \sqrt{\sum_{i,j}\left[W_{ij}^{EE}(t) - W_{ij}^{EE}(t-dt)\right]^2}/{N_E}^2 \qquad (15)$$

$$\Delta \boldsymbol{W}^{\mathrm{EI}}(t) \coloneqq \sqrt{\sum_{i,j}\left[W_{ij}^{EI}(t) - W_{ij}^{EI}(t-dt)\right]^2}/(N_E N_I), \qquad (16)$$

where $W_{ij}^{Ea}(t)\ (a = E; I)$ is a synapse at time t and dt is a simulation time step of 1 ms.

Calculation of error dynamics in task switching

In Supplementary Figures 3c and 3d, two types of prediction errors for excitatory and inhibitory plasticity were calculated as follows. First, we obtained the low-pass filtered errors $\mathcal{E}_i^{\mathrm{exc}}$ and $\mathcal{E}_i^{\mathrm{inh}}$ calculated by instantaneous error values in the plasticity rules (i.e., Eqs. 11 and 13) as:

$$\tau_{\mathrm{avg}}\dot{\mathcal{E}}_i^{\mathrm{exc}} = -\mathcal{E}_i^{\mathrm{exc}} + [f_i^{\mathrm{E}}(t) - y_i^{\mathrm{E}}(t)] \qquad (17)$$

$$\tau_{\mathrm{avg}}\dot{\mathcal{E}}_i^{\mathrm{inh}} = -\mathcal{E}_i^{\mathrm{inh}} + \left[y_i^{\mathrm{E}}(t) - y_i^{\mathrm{I}}(t)\right], \qquad (18)$$

where $\tau_{\mathrm{avg}} = 30$ s is a time constant for low-pass filter and i is a neuron index. We then calculated the averaged errors $\mathrm{PE}^{\mathrm{exc}}$ and $\mathrm{PE}^{\mathrm{inh}}$ as:

$$\mathrm{PE}^{\mathrm{exc}}(t) = \frac{1}{N_E}\sum_{i=1}^{N_E}|\mathcal{E}_i^{\mathrm{exc}}(t)| \qquad (19)$$

$$\mathrm{PE}^{\mathrm{inh}}(t) = \frac{1}{N_E}\sum_{i=1}^{N_E}\left|\mathcal{E}_i^{\mathrm{inh}}(t)\right|, \qquad (20)$$

where $|\cdot|$ is an absolute value.

Analysis of the low-dimensional representation in network

In Fig.4h, we first obtained matrix of network responses $U = (\boldsymbol{r}_1, \ldots, \boldsymbol{r}_{15})$, where $\boldsymbol{r}_i$ $(i = 1, \ldots, 15)$ is a trial-averaged response of a whole network to one of 15 stimulus patterns shown in Fig.4d. Trial averaging was performed over multiple presentations of each stimulus. We then applied the principal component analysis (PCA) to matrix U and visualized the low dimensional representation of multiple stimulus in the learned network.

Correlation measure for comparison with a songbird

In Fig 5, we calculated stimulus-triggered averages of autonomous network activity to obtain poststimulus activity (PSA) of a network model. In Figs 5b and 5c, correlation between PSA and evoked activity triggered by one stimulus pattern was calculated neuron-wise and then averaged over all neurons.

Acknowledgments

This work was supported by BBSRC (BB/N013956/1), Wellcome Trust (200790/Z/16/Z), the Simons Foundation (564408) and EPSRC(EP/R035806/1). The authors also thank Ian Cone for his comments on the manuscript and technical assistance.

References

1. Amit DJ, Brunel N. Model of global spontaneous activity and local structured activity during delay periods in the cerebral cortex. Cereb Cortex. 1997 Apr-May;7(3):237-52. doi: 10.1093/cercor/7.3.237. PMID: 9143444.
2. Asabuki T, Fukai T. Somatodendritic consistency check for temporal feature segmentation. Nat Commun. 2020 Mar 25;11(1):1554. doi: 10.1038/s41467-020-15367-w. PMID: 32214100; PMCID: PMC7096495.
3. Baddeley A. Working memory. Science. 1992 Jan 31;255(5044):556-9. doi: 10.1126/science.1736359. PMID: 1736359.
4. Barak O, Tsodyks M. Working models of working memory. Curr Opin Neurobiol. 2014 Apr;25:20-4. doi: 10.1016/j.conb.2013.10.008. Epub 2013 Dec 4. PMID: 24709596.

5. Bell C, Bodznick D, Montgomery J, Bastian J. The generation and subtraction of sensory expectations within cerebellum-like structures. Brain Behav Evol. 1997;50 Suppl 1:17-31. doi: 10.1159/000113352. PMID: 9217991.
6. Berkes, P., Orban, G., Lengyel, M. & Fiser, J. Spontaneous cortical activity reveals hallmarks of an optimal internal model of the environment. Science 331, 83-87 (2011).
7. Berman GJ, Bialek W, Shaevitz JW. Predictability and hierarchy in Drosophila behavior. Proceedings of the National Academy of Sciences of the United States of America. 2016; 113(42):11943–11948. https://doi.org/10.1073/pnas.1607601113 PMID: 27702892
8. Bouchard KE, Brainard MS. Auditory-induced neural dynamics in sensory-motor circuitry predict learned temporal and sequential statistics of birdsong. Proc Natl Acad Sci U S A. 2016 Aug 23;113(34):9641-6. doi: 10.1073/pnas.1606725113. Epub 2016 Aug 9. PMID: 27506786; PMCID: PMC5003256.
9. Brea J, Senn W, Pfister JP. Matching Recall and Storage in Sequence Learning with Spiking Neural Networks. Journal of Neuroscience. 2013; 33(23):9565–9575. https://doi.org/10.1523/JNEUROSCI. 4098-12.2013 PMID: 23739954
10. Chadwick A, van Rossum MC, Nolan MF. Independent theta phase coding accounts for CA1 population sequences and enables flexible remapping. Elife. 2015 Feb 2;4:e03542. doi: 10.7554/eLife.03542. PMID: 25643396; PMCID: PMC4383210.
11. D'amour JA, Froemke RC. Inhibitory and excitatory spike-timing-dependent plasticity in the auditory cortex. Neuron. 2015 Apr 22;86(2):514-28. doi: 10.1016/j.neuron.2015.03.014. Epub 2015 Apr 2. PMID: 25843405; PMCID: PMC4409545.
12. Davidson TJ, Kloosterman F, Wilson MA. Hippocampal replay of extended experience. Neuron. 2009 Aug 27;63(4):497-507. doi: 10.1016/j.neuron.2009.07.027. PMID: 19709631; PMCID: PMC4364032.
13. Diba K, Buzsáki G. Forward and reverse hippocampal place-cell sequences during ripples. Nat Neurosci. 2007 Oct;10(10):1241-2. doi: 10.1038/nn1961. Epub 2007 Sep 2. PMID: 17828259; PMCID: PMC2039924.
14. Erickson MA, Maramara LA, Lisman J. A single brief burst induces GluR1-dependent associative short-term potentiation: a potential mechanism for

short-term memory. J Cogn Neurosci. 2010 Nov;22(11):2530-40. doi: 10.1162/jocn.2009.21375. PMID: 19925206; PMCID: PMC3195522.

15. Fonollosa J, Neftci E, Rabinovich M. Learning of Chunking Sequences in Cognition and Behavior. PLoS Comput Biol. 2015 Nov 19;11(11):e1004592. doi: 10.1371/journal.pcbi.1004592. PMID: 26584306; PMCID: PMC4652905.
16. Funahashi S, Bruce CJ, Goldman-Rakic PS. Mnemonic coding of visual space in the monkey's dorsolateral prefrontal cortex. J Neurophysiol. 1989 Feb;61(2):331-49. doi: 10.1152/jn.1989.61.2.331. PMID: 2918358.
17. Fuster JM, Alexander GE. Neuron activity related to short-term memory. Science. 1971 Aug 13;173(3997):652-4. doi: 10.1126/science.173.3997.652. PMID: 4998337.
18. Gabriel Koch Ocker, Brent Doiron, Training and Spontaneous Reinforcement of Neuronal Assemblies by Spike Timing Plasticity, *Cerebral Cortex*, Volume 29, Issue 3, March 2019, Pages 937–951, https://doi.org/10.1093/cercor/bhy001
19. Geddes CE, Li H, Jin X. Optogenetic Editing Reveals the Hierarchical Organization of Learned Action Sequences. Cell. 2018; 174(1):32–43.e15. https://doi.org/10.1016/j.cell.2018.06.012 PMID: 29958111
20. Goldman-Rakic PS. Cellular basis of working memory. Neuron. 1995 Mar;14(3):477-85. doi: 10.1016/0896-6273(95)90304-6. PMID: 7695894.
21. Gupta AS, van der Meer MA, Touretzky DS, Redish AD. Hippocampal replay is not a simple function of experience. Neuron. 2010 Mar 11;65(5):695-705. doi: 10.1016/j.neuron.2010.01.034. PMID: 20223204; PMCID: PMC4460981.
22. Jin X, Costa RM. Shaping action sequences in basal ganglia circuits. Current Opinion in Neurobiology. 2015; 33:188–196. https://doi.org/10.1016/j.conb.2015.06.011 PMID: 26189204
23. Jovanic T, Schneider-Mizell CM, Shao M, Masson JB, Denisov G, Fetter RD, et al. Competitive Disinhi- bition Mediates Behavioral Choice and Sequences in Drosophila. Cell. 2016; 167(3):858–870.e19. https://doi.org/10.1016/j.cell.2016.09.009 PMID: 27720450
24. Kaplan HS, Salazar Thula O, Khoss N, Zimmer M. Nested Neuronal Dynamics Orchestrate a Behav- ioral Hierarchy across Timescales. Neuron. 2020; 105(3):562–576.e9. https://doi.org/10.1016/j.neuron. 2019.10.037 PMID: 31786012
25. Katahira K, Suzuki K, Okanoya K, Okada M. Complex sequencing rules of birdsong can be explained by simple hidden Markov processes. PLoS One.

2011;6(9):e24516. doi: 10.1371/journal.pone.0024516. Epub 2011 Sep 7. PMID: 21915345; PMCID: PMC3168521.

26. Kato S, Kaplan HS, Schro¨del T, Skora S, Lindsay TH, Yemini E, et al. Global Brain Dynamics Embed the Motor Command Sequence of Caenorhabditis elegans. Cell. 2015; 163(3):656–669. https://doi.org/10.1016/j.cell.2015.09.034 PMID: 26478179
27. Kempter R, Gerstner W, van Hemmen JL (1999) Hebbian learning and spiking neurons. Physical Review E 59: 4498–4514.
28. Kogan JA, Margoliash D. Automated recognition of bird song elements from continuous recordings using dynamic time warping and hidden Markov models: a comparative study. J Acoust Soc Am. 1998 Apr;103(4):2185-96. doi: 10.1121/1.421364. PMID: 9566338.
29. Lee A.K., Wilson M.A. Memory of sequential experience in the hippocampus during slow wave sleep. Neuron. 2002;36:1183–1194. [PubMed] [Google Scholar]
30. Levy N, Horn D, Meilijson I, Ruppin E. Distributed synchrony in a cell assembly of spiking neurons. Neural Netw. 2001 Jul-Sep;14(6-7):815-24. doi: 10.1016/s0893-6080(01)00044-2. PMID: 11665773.
31. Lewald J, Ehrenstein WH. Influence of head-to-trunk position on sound lateralization. Exp Brain Res. 1998 Aug;121(3):230-8. doi: 10.1007/s002210050456. PMID: 9746129.
32. Litwin-Kumar, A., Doiron, B. Formation and maintenance of neuronal assemblies through synaptic plasticity. *Nat Commun* **5**, 5319 (2014). https://doi.org/10.1038/ncomms6319
33. Markowitz JE, Gillis WF, Beron CC, Neufeld SQ, Robertson K, Bhagat ND, et al. The Striatum Orga- nizes 3D Behavior via Moment-to-Moment Action Selection. Cell. 2018; 174(1):44–58.e17. https://doi.org/10.1016/j.cell.2018.04.019 PMID: 29779950
34. Masquelier T, Guyonneau R, Thorpe SJ (2008) Spike timing dependent plasticity finds the start of repeating patterns in continuous spike trains. PLoS One 3: e1377.
35. Merfeld DM, Zupan L, Peterka RJ. Humans use internal models to estimate gravity and linear acceleration. Nature. 1999 Apr 15;398(6728):615-8. doi: 10.1038/19303. PMID: 10217143.

36. Miller EK, Cohen JD. An integrative theory of prefrontal cortex function. Annu Rev Neurosci. 2001;24:167-202. doi: 10.1146/annurev.neuro.24.1.167. PMID: 11283309.
37. Mongillo G, Barak O, Tsodyks M. Synaptic theory of working memory. Science. 2008 Mar 14;319(5869):1543-6. doi: 10.1126/science.1150769. PMID: 18339943.
38. Pfister JP, Toyoizumi T, Barber D, Gerstner W. Optimal spike-timing-dependent plasticity for precise action potential firing in supervised learning. Neural Comput. 2006 Jun;18(6):1318-48. doi: 10.1162/neco.2006.18.6.1318. PMID: 16764506.
39. Pudhiyidath A, Morton NW, Viveros Duran R, Schapiro AC, Momennejad I, Hinojosa-Rowland DM, Molitor RJ, Preston AR. Representations of Temporal Community Structure in Hippocampus and Precuneus Predict Inductive Reasoning Decisions. J Cogn Neurosci. 2022 Sep 1;34(10):1736-1760. doi: 10.1162/jocn_a_01864. PMID: 35579986.
40. Schapiro AC, Rogers TT, Cordova NI, Turk-Browne NB, Botvinick MM. Neural representations of events arise from temporal community structure. Nat Neurosci. 2013 Apr;16(4):486-92. doi: 10.1038/nn.3331. Epub 2013 Feb 17. PMID: 23416451; PMCID: PMC3749823.
41. Seeds AM, Ravbar P, Chung P, Hampel S, Midgley FM, Mensh BD, et al. A suppression hierarchy among competing motor programs drives sequential grooming in Drosophila. eLife. 2014; 3:e02951. https://doi.org/10.7554/eLife.02951 PMID: 25139955
42. Skaggs W.E., McNaughton B.L. Replay of neuronal firing sequences in rat hippocampus during sleep following spatial experience. Science. 1996;271:1870–1873. [PubMed] [Google Scholar]
43. Song S, Miller KD, Abbott LF (2000) Competitive Hebbian learning through spike-timing dependent synaptic plasticity. Nature Neuroscience 3: 919–926.
44. Toshitake Asabuki and Tomoki Fukai. Learning rules for cortical-like spontaneous replay of an internal model. bioRxiv 2023.02.17.528958; doi: https://doi.org/10.1101/2023.02.17.528958
45. Triplett MA, Avitan L, Goodhill GJ (2018) Emergence of spontaneous assembly activity in developing neural networks without afferent input. PLOS Computational Biology 14(9): e1006421. https://doi.org/10.1371/journal.pcbi.1006421

46. Urbanczik R, Senn W. Learning by the dendritic prediction of somatic spiking. Neuron. 2014 Feb 5;81(3):521-8. doi: 10.1016/j.neuron.2013.11.030. PMID: 24507189.
47. Vogels TP, Sprekeler H, Zenke F, Clopath C, Gerstner W. Inhibitory plasticity balances excitation and inhibition in sensory pathways and memory networks. Science. 2011 Dec 16;334(6062):1569-73. doi: 10.1126/science.1211095. Epub 2011 Nov 10. Erratum in: Science. 2012 May 18;336(6083):802. PMID: 22075724.
48. Wilson M.A., McNaughton B.L. Reactivation of hippocampal ensemble memories during sleep. Science. 1994;265:676–679. [PubMed] [Google Scholar]
49. Wolpert DM, Ghahramani Z, Jordan MI. An internal model for sensorimotor integration. Science. 1995 Sep 29;269(5232):1880-2. doi: 10.1126/science.7569931. PMID: 7569931.
50. Wu X, Foster DJ. Hippocampal replay captures the unique topological structure of a novel environment. J Neurosci. 2014 May 7;34(19):6459-69. doi: 10.1523/JNEUROSCI.3414-13.2014. PMID: 24806672; PMCID: PMC4012305.
51. Yasui S, Young LR. Perceived visual motion as effective stimulus to pursuit eye movement system. Science. 1975 Nov 28;190(4217):906-8. doi: 10.1126/science.1188373. PMID: 1188373.
52. Zucker RS, Regehr WG. Short-term synaptic plasticity. Annu Rev Physiol. 2002;64:355-405. doi: 10.1146/annurev.physiol.64.092501.114547. PMID: 11826273.